# Supporting Information

## Oja et al. 10.1073/pnas.1207407110

### SI Text

**Purification and Structural Elucidation of Alnumycins P1 (4a) and P2 (4b).** For preparative production of alnumycins P1 (**4a**) and P2 (**4b**), 60 0.4-mL analytical-scale AlnA reactions consisting of 75 mM D-ribose-5-phosphate, 0.5 mM prealnumycin (**2**), and 23 μM AlnA were incubated for 3 h at 288 K. After incubation, the combined mixtures were acidified with 2.5% (vol/vol) HCOOH, centrifuged, and applied to Sep-Pak PLUS C18 cartridges (Millipore, Waters) preequilibrated with 0.1% (vol/vol) HCOOH and eluted with methanol. The reaction extracts in methanol were then applied to a Discovery HSC18 column (5 μm, 5 cm × 4.6 mm; Supelco) and eluted with 20 mM aqueous ammonium acetate pH 3.6 and a 70–100% (vol/vol) methanol gradient to yield 0.5 mg of alnumycin P (**4**), ∼50% pure by HPLC and NMR. For all other HPLC columns tested, the chromatographic behavior of **4** was exceedingly poor as the sample appeared to be strongly retained on the columns with only minor amounts of material eluting over extended periods of time even when using 100% (vol/vol) organic solvent. Unfortunately, the compound degraded readily in aqueous environments complicating its further purification.

The structural elucidation of **4** followed from $ESI^-$-HR-MS, which provided an accurate mass of 495.1059 amu for the M − 1 ion alluding to a molecular formula of $C_{22}H_{25}O_{11}P$ (calculated for the M − 1 ion, 495.1062 amu). The presence of an intact prealnumycin moiety was inferred by the observation of (*i*) a chromophore in UV-vis spectroscopy pertaining to such and (*ii*) various protons and carbons (Table S3) that were consistent to previous observations of the prealnumycin moiety with regard to both chemical shift and multiplicity (1, 2). Because of the limited sample amount, direct observation of carbon was not possible, and only indirect observation of the carbons was amenable via heteronuclear single quantum coherence (HSQC) and heteronuclear multiple bond correlation (HMBC) spectroscopy.

The inclusion of phosphorous in **4** as indicated by HR-MS was readily confirmed by $^{31}P$ NMR. The presence of a phosphate group combined with a sugar residue—thus a highly polar entity—was also strongly implied by the aberrant chromatographic behavior and extraction properties (viz. negligible solubility in chloroform and water and only ready solubility in methanol) exhibited by the compound. The HR-MS result also implied the presence of a ring-closed ribose unit attached to a prealnumycin moiety with an attendant phosphate group, presumably attached to the ribose unit, to account fully for the molecular formula. Indeed, a ribose unit in the furanose form with both β (**4a**, major isomer, 83.9%) and α (**4b**, 16.1%) anomers present in the sample was clearly indicated by $^1H$ NMR, with chemical shifts and couplings for the signals of H-1′ akin to the analogous H-1′ signals observed in alnumycins C1 (**3a**) and C2 (**3b**) (2), respectively. Although only one distinct $^{31}P$ NMR signal was forthcoming, its multiplicity was determined to be a triplet ($J \sim 5.8$ Hz) by coupled acquisition, as analysis of the $^1H\{^{31}P\}$-HMBC spectrum was compromised by the extensive overlap of the $^1H$ signals in the sugar residue. Thus, the positioning of the phosphate group at C-5′ in both **4a** and **4b** was based on this coupling together with the knowledge that O-4′ must be blocked due to the furanose ring formation and the chemical shifts and couplings, where observable, of H-1′, H-2′, and H-3′ did not indicate phosphate attachment to the pertinent oxygens. Finally, the attachment of the furanose ring to C-8 of the prealnumycin skeleton and the attachment of the prealnumycin moiety to C-1′ of the ribose unit were evident by the long-range coupling between H-7 and H-1′ by long-range correlation spectroscopy (COSY) and decoupling experiments.

Of note, neither **3a** nor **3b** was discerned to be present in the sample by $^1H$ NMR, nor was any open-chain form of the ribose unit in effect based on the integration of the $^1H$ signals, e.g., H-1′ and H-7 with respect to H-4. Furthermore, additional $^{31}P$ NMR signals were not observed, thereby precluding the presence of any free phosphate in the sample.

**Binding of D-Ribulose-5-Phosphate to AlnA.** The binding of D-ribulose-5-phosphate to AlnA was studied by transfer of bulk water magnetization to the ligand (3, 4). The NMR samples consisted of the following: 4 mM D-ribulose-5-phosphate and 428 (124) μM AlnA in 12.5 mM $H_3PO_4$ (pH 6.85), 37.5 mM NaCl, 1.25 mM $MgCl_2$, 15% (vol/vol) glycerol, 5% (vol/vol) $D_2O$, and 1 mM DMSO to yield substrate to protein ratios of 9.3:1 (32:1) (Fig. S5) and 2 mM D-ribulose-5-phosphate and 33.6 μm AlnA in a similar solution to yield a substrate to protein ratio of 60:1. To prevent the possible spontaneous oxidation of the substrates, the samples were bubbled for ∼10 min with 99.999% (vol/vol) argon gas and stored under argon. Control samples lacking the protein were prepared in an otherwise identical fashion. All samples were prepared and stored on ice. The waterLOGSY spectra were acquired using the pulse sequence of Dalvit (3, 4) and with an *Aq* of 1.64 s, 3.8 s for the postacquisition delay (PAD), and a mixing time ($\tau_m$) of 750 ms; suppression of the water signal was effected by excitation sculpting (5) using a 2-ms sinc-shaped pulse, whereas selective excitation of the water signal was effected by a 5-ms Gaussian-shaped pulse; spectra were processed with zero-filling (×4) and the application of 2 Hz of line broadening.

**Crystallization of AlnA and AlnB.** The proteins AlnA and AlnB were produced and purified as described previously (2). For AlnA, diffraction quality cubic crystals were obtained by mixing 2 μL of AlnA (7 mg/mL) in 25 mM Hepes (pH 7.2), 75 mM NaCl, 5% glycerol, and 5 mM $MgCl_2$ together with 1 μL of well solution containing 100 mM malonic acid–imidazole–boric acid (MIB) buffer (pH 7.2), 200 mM calcium acetate, and 20% (vol/vol) PEG3000 at 277 K. Thick rod shape crystals of AlnB were obtained by mixing 1 μL of AlnB (13 mg/mL) in 50 mM Hepes (pH 7.2), 150 mM NaCl, 10 mM $MgCl_2$, and 10% (vol/vol) glycerol together with 2 μL of well solution, which consisted of 30% (vol/vol) PEG1500 and 100 mM MIB buffer (pH 7.0) at 277 K. The native crystals were cryo-protected by quick soaking in mother liquor supplemented with 20% (vol/vol) (AlnA) or 25% (vol/vol) (AlnB) PEG600 and flash frozen at 100 K. The phosphate complex of AlnB was obtained by adding 10 mM sodium phosphate into the cryo solution. The D-ribose-5-phosphate complex of AlnA was obtained by soaking the crystal for 40 min in a cryo solution containing 100 mM MIB buffer (pH 7.2), 25% (vol/vol) PEG3000, 100 mM D-ribose-5-phosphate, and 20% (vol/vol) PEG400.

**Generation of AlnA and AlnB Enzyme Variants.** AlnA variants K86A, H130A, and K159A were prepared using the plasmid pBla7AB (1) as a template. The first round of PCR was accomplished with the primer AlnAmutfor with each reverse mutagenesis primer and AlnAmutrev with each forward mutagenesis primer (Table S2). PCR products isolated from a preparative agarose gel were used as templates for the second round of PCR with AlnAmutfor and -rev as a primer pair, and the product fragments were digested with Eco81I and PaeI and cloned into a similarly digested pBla7AB. For protein overexpression, the constructs were di-

gested with SgrAI and Bpu1102I and cloned into a similarly digested pBADHBdaA (2).

For generation of AlnA variants E29A, E29Q, D138A, and K159R, a similar four-primer approach was used with pBADHBdaA (2) as a template in the first round of PCR. The forward sequencing primer pBADseqfor was used with each reverse mutagenesis primer, and pBADseqrev with each forward mutagenesis primer (Table S2). The PCR products were isolated and used as templates for the second round of PCR with pBADseqfor and -rev as a primer pair. The products were then digested with NcoI and HindIII and cloned into a similarly digested pBADHBd (6).

The AlnB variants D17A, K119A, and K119R were prepared using the plasmid pBla7AB (1) as a template. The first round of PCR was accomplished with the primer pBla7ABfor together with each reverse mutagenesis primer and pBla7ABrev with each forward mutagenesis primer (Table S2). The PCR products isolated from a preparative agarose gel were used as templates for the second round of PCR with pBla7ABfor and -rev as a primer pair. The product fragments were digested with PaeI and XbaI and cloned into a similarly digested pBla7AB and further as XbaI + HindIII digested insert fragments into a similarly digested pIJ487 vector (7). The plasmid DNA isolated from *Streptomyces lividans* TK24 was then used as a PCR template with alnBBfor and alnBErev as a primer pair, and the BglII + EcoRI digested PCR products were finally cloned into a similarly digested pBADHBd.

The AlnB variants D15A, D15N, and Y79A were prepared using the protein production construct pBADHBdaB (2) as a template. The pBADseqfor sequencing primer was used with the reverse mutagenesis primers D15Arev and D15Nrev, whereas alnBBfor was used with the Y79Arev primer and the alnBErev primer with each forward mutagenesis primer (Table S2) for the first round of PCR. With the isolated PCR products as templates, the second round was accomplished using alnBBfor and alnBErev as primers. The PCR products were again digested with BglII and EcoRI and cloned into a similarly digested pBADHBd.


1. Oja T, et al. (2008) Characterization of the alnumycin gene cluster reveals unusual gene products for pyran ring formation and dioxan biosynthesis. *Chem Biol* 15(10):1046–1057.
2. Oja T, et al. (2012) Biosynthetic pathway toward carbohydrate-like moieties of alnumycins contains unusual steps for C-C bond formation and cleavage. *Proc Natl Acad Sci USA* 109(16):6024–6029.
3. Dalvit C (1996) Homonuclear 1D and 2D NMR experiments for the observation of solvent-solute interactions. *J Magn Reson B* 112(3):282–288.
4. Dalvit C, et al. (2000) Identification of compounds with binding affinity to proteins via magnetization transfer from bulk water. *J Biomol NMR* 18(1):65–68.
5. Hwang T-L, Shaka AJ (1995) Water suppression that works. Excitation sculpting using arbitrary waveforms and pulsed field gradients. *J Magn Reson A* 112:275–279.
6. Kallio P, Sultana A, Niemi J, Mäntsälä P, Schneider G (2006) Crystal structure of the polyketide cyclase AknH with bound substrate and product analogue: Implications for catalytic mechanism and product stereoselectivity. *J Mol Biol* 357(1):210–220.
7. Hopwood DA, et al. (1985) *Genetic Manipulation of Streptomyces: A Laboratory Manual* (John Innes Foundation, Norwich, UK).


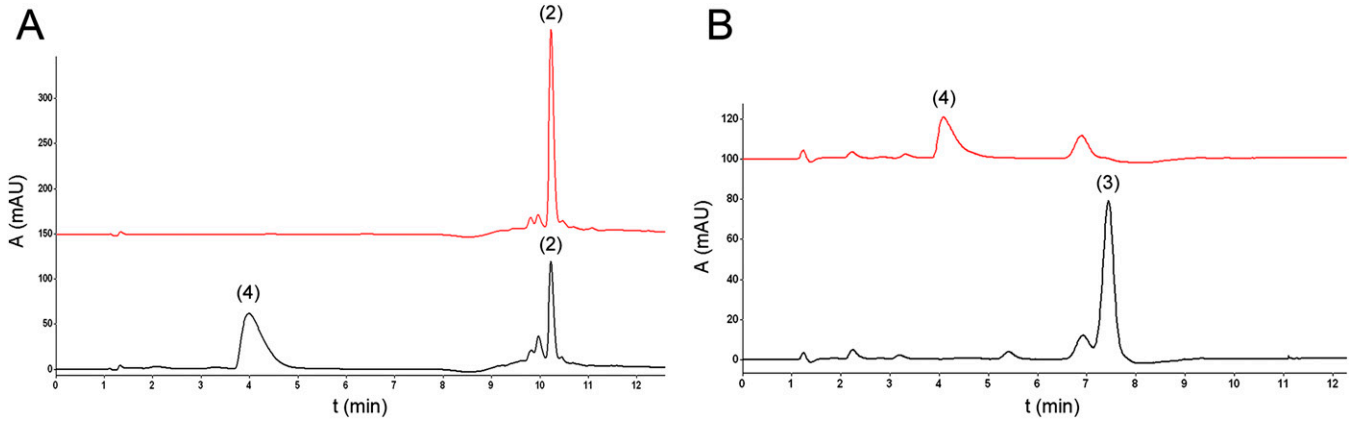


**Fig. S1.** Enzymatic synthesis of (*A*) alnumycin P (**4**) from 100 mM D-ribose-5-phosphate and 1 mM prealnumycin (**2**) by 15 μM AlnA (3 h incubation) and (*B*) enzymatic conversion of **4** to alnumycin C (**3**) by 4 μM AlnB (1-h incubation). In both cases, a parallel control reaction with boiled enzyme is shown in red. All HPLC traces shown are recorded at 470 nm.

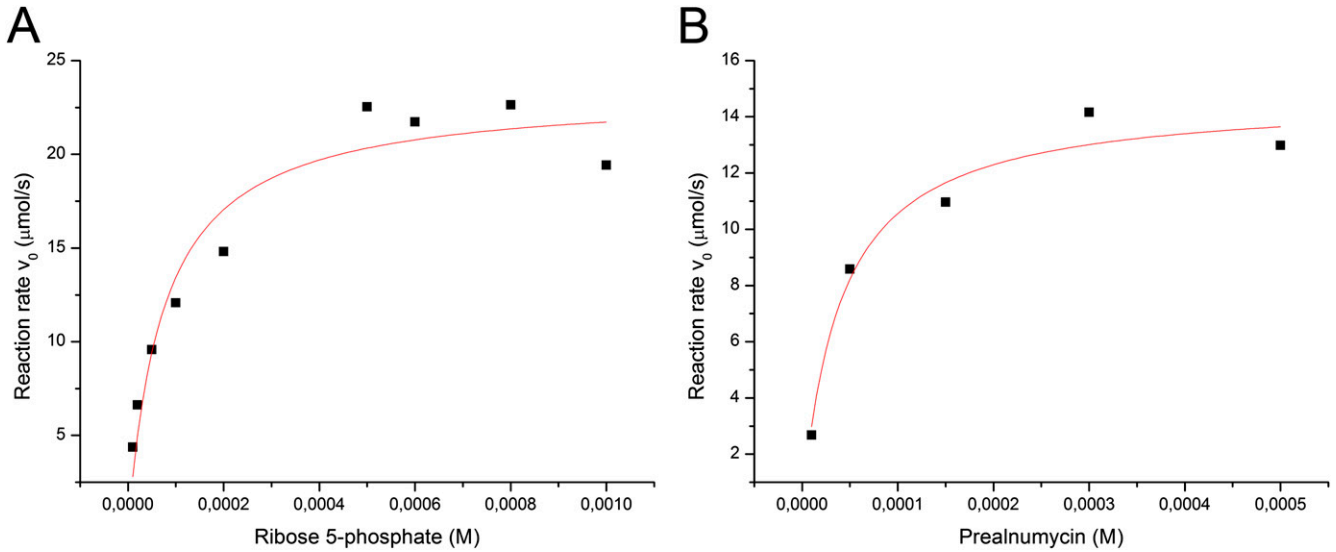


**Fig. S2.** Kinetic analysis of the AlnA reaction in regards to the utilization of (*A*) D-ribose-5-phosphate and (*B*) prealnumycin (**2**). The kinetic parameters extracted from the data were as follows: D-ribose-5-phosphate, apparent $K_m$ = 74 ± 19 μM, $k_{cat}$ = 0.58 ± 0.03 $s^{-1}$ and $K_m/k_{cat}$ = 7900 $M^{-1}$ $s^{-1}$; prealnumycin, apparent $K_m$ = 39 ± 11 μM, $k_{cat}$ = 0.37 ± 0.02 $s^{-1}$ and $K_m/k_{cat}$ = 9300 $M^{-1}$ $s^{-1}$.

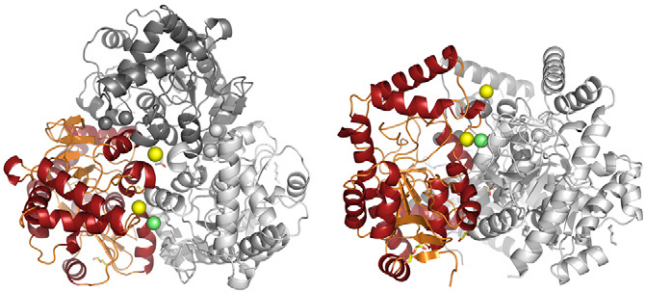

**Fig. S3.** Quaternary structure of the trimeric AlnA. (*Left*) Top view. (*Right*) Side view. One subunit is shown in red α-helices and orange β-sheets with $Ca^{2+}$ and $Cl^-$ ions in yellow and green, respectively. The two other subunits are depicted in gray and light gray. Analysis with the protein interfaces, surfaces, and assemblies service (PISA) at the European Bioinformatics Institute (1) indicates that the AlnA trimer assembly with the embedded ions is stable in solution. The total buried surface area is 9,490 $Å^2$, and the calculated solvation free energy gain (Δ*G*) on formation of the assembly is −136 kcal/mol. There are seven intersubunit hydrogen bonds per interface in addition to the interactions coordinating the bound ions.

1. Krissinel E, Henrick K (2007) Inference of macromolecular assemblies from crystalline state. *J Mol Biol* 372(3):774–797.

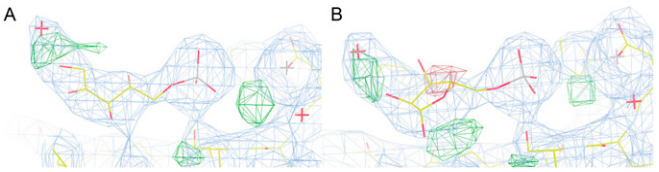


**Fig. S4.** Refined models of (*A*) linear D-ribulose-5-phosphate and (*B*) cyclic D-ribose-5-phosphate built into the electron density of AlnA-5RP. The 2Fo-Fc (blue) and Fo-Fc (red, negative density; green, positive density) electron density maps have been contoured at 1.5 and 3.0 σ, respectively.

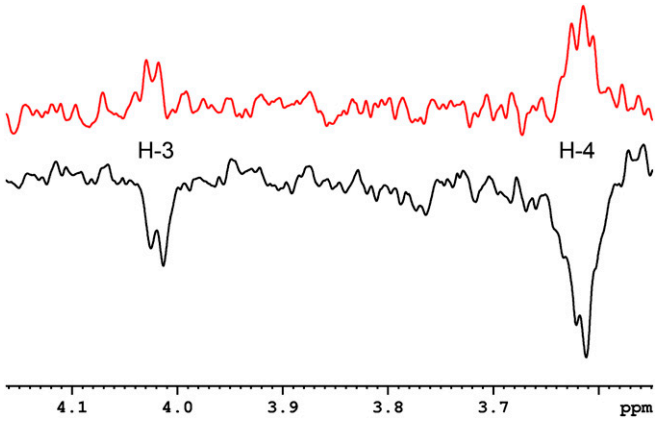


**Fig. S5.** Binding of D-ribulose-5-phosphate to AlnA as demonstrated by waterLOGSY (1, 2). The opposite sign of the NMR resonances in the measurement of D-ribulose phosphate with AlnA (black) in contrast to the control reaction without AlnA (red) indicates binding. The region covering the H-3 and H-4 protons is shown in the magnification because signals originating from the two H-1 and the two H-5 protons of D-ribulose-5-phosphate were overlapping with $H_2O$ and glycerol, respectively.

1. Dalvit C (1996) Homonuclear 1D and 2D NMR Experiments for the Observation of Solvent-Solute Interactions. *J Magn Reson B* 112(3):282–288.
2. Dalvit C, et al. (2000) Identification of compounds with binding affinity to proteins via magnetization transfer from bulk water. *J Biomol NMR* 18(1):65–68.

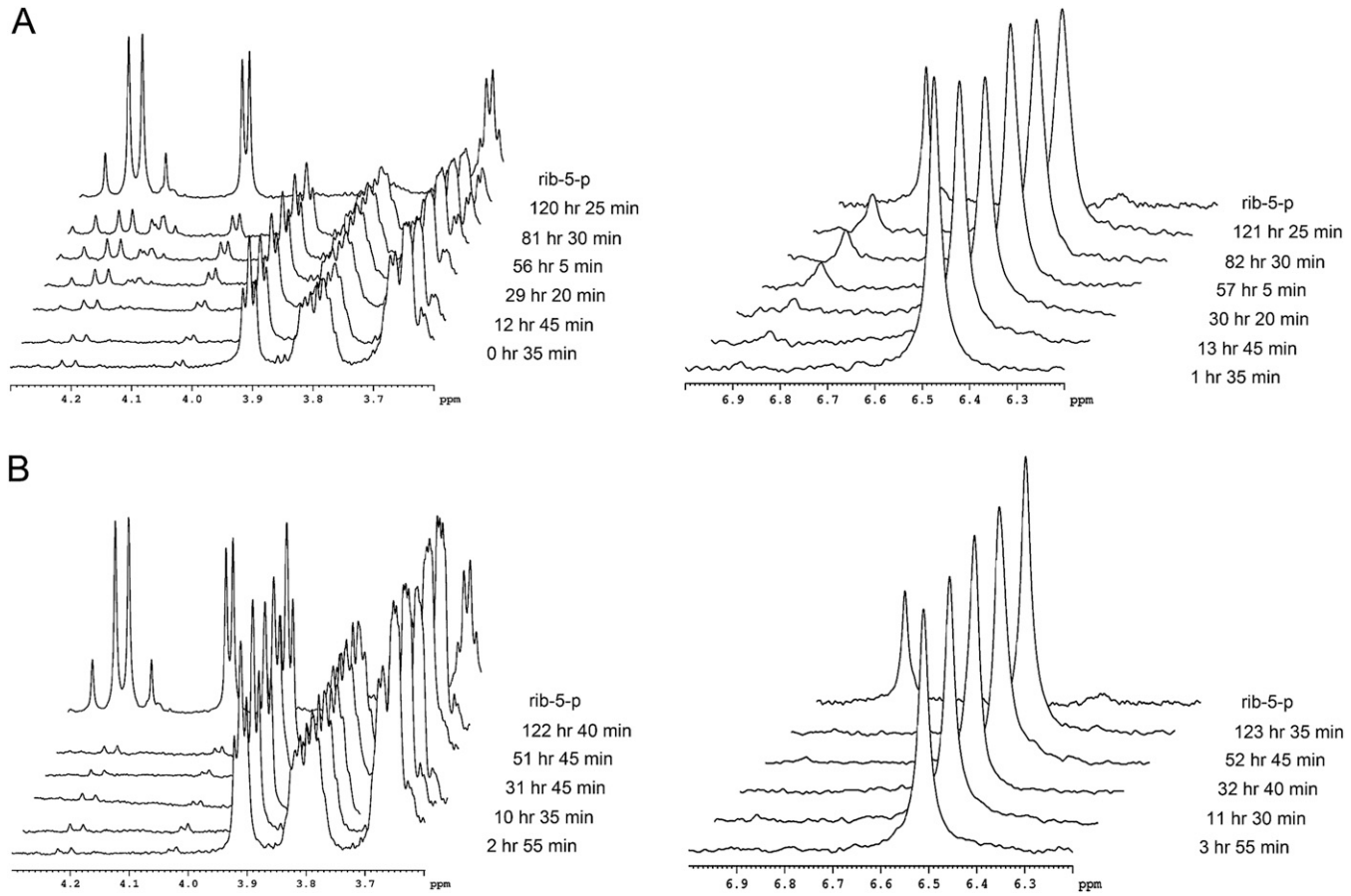


**Fig. S6.** Conversion of D-ribose-5-phosphate into D-ribulose-5-phosphate by AlnA. Time-course of the $^{1}H$ and $^{31}P$ spectra for 4 mM D-ribose-5-phosphate (*A*) in the presence of 124 μM AlnA and (*B*) in the absence of AlnA. Legend: rib-5-p, D-ribulose-5-phosphate control.

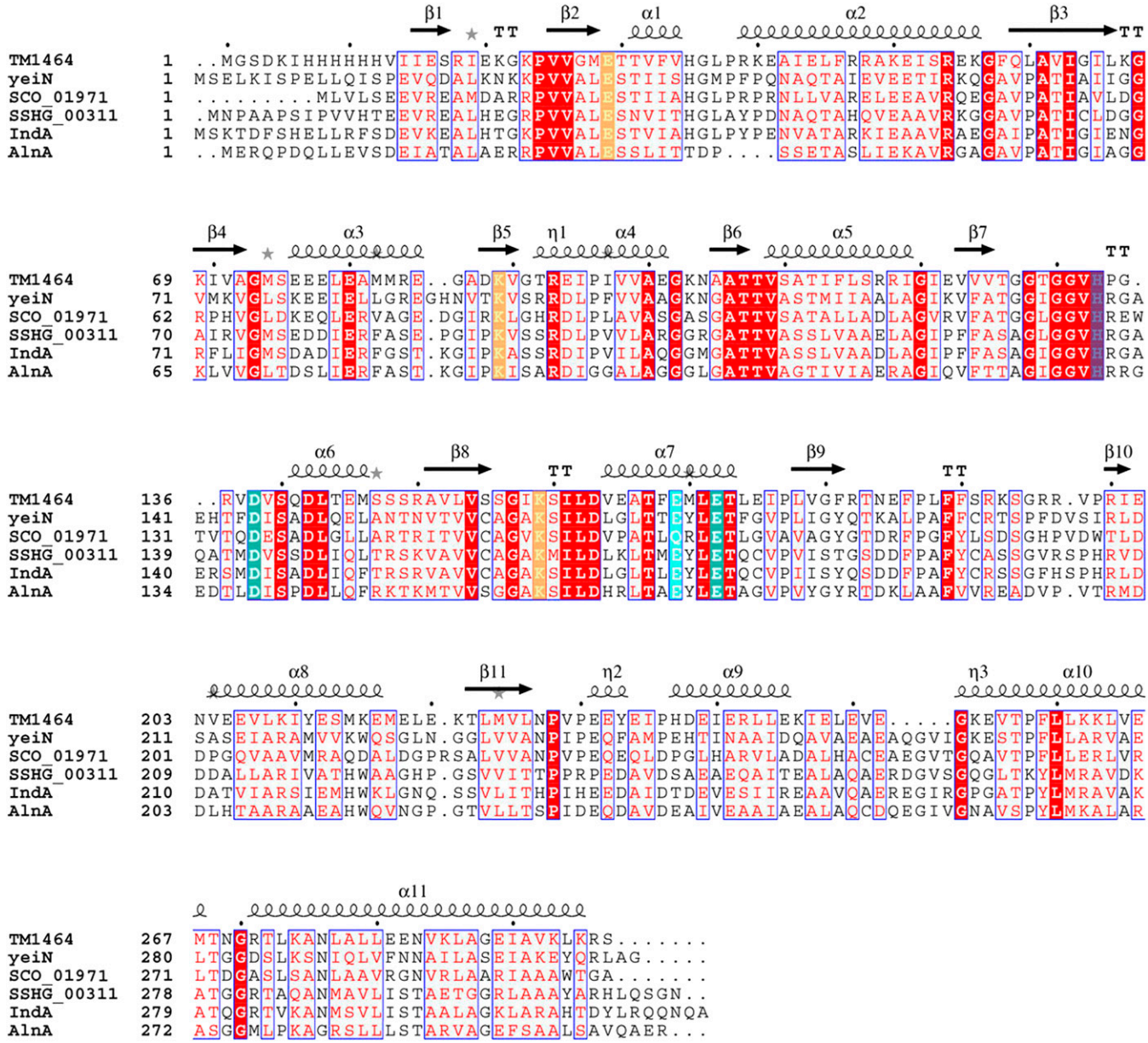


**Fig. S7.** Structure-based multiple sequence alignment of AlnA with related homologous enzymes. The proteins are pseudouridine glycosidase TM1464, *Thermotoga maritima*; pseudouridine glycosidase YeiN, *Escherichia coli*; protein of unknown function SCO_01971, *S. coelicolor*; protein of unknown function SSHG_00311, *S. albus* and protein putatively involved in the biosynthesis of the pigment indigoidine IndA, *Erwinia chrysanthemi*. Amino acid residues that are conserved (red line), involved in catalysis (orange line), coordinating to the metal ion (cyan line), or the phosphate group of the cosubstrate (purple line) are shown.

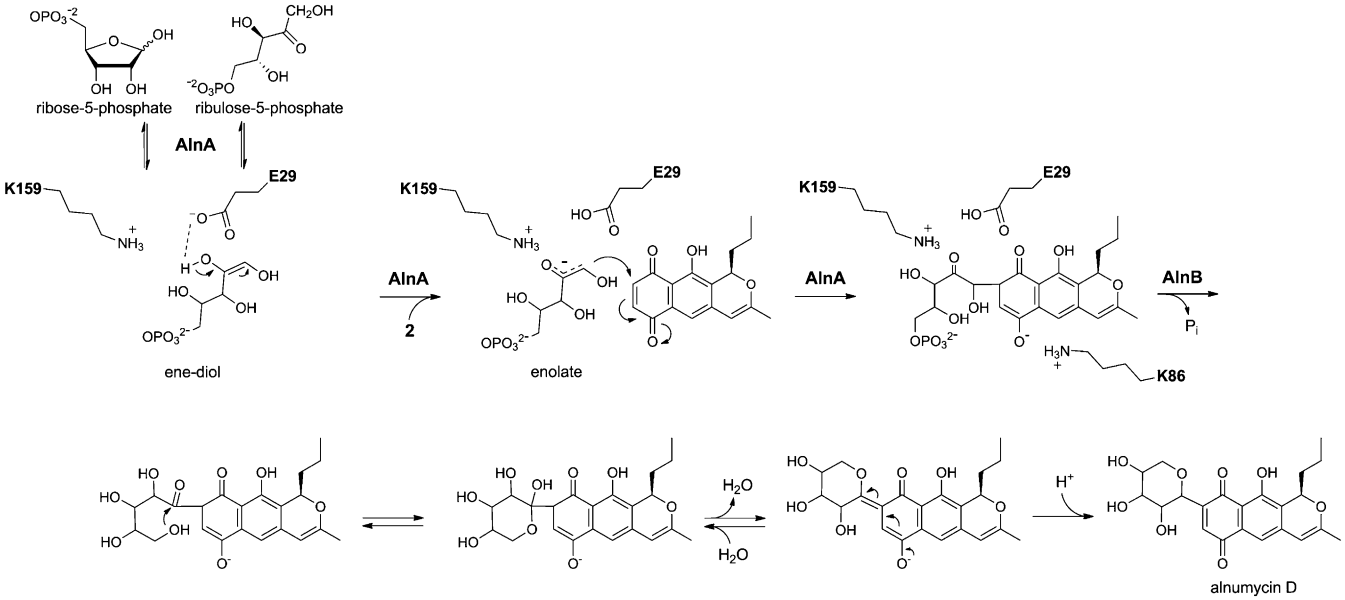


**Fig. S8.** Mechanistic model for formation of the shunt product alnumycin D by AlnA and AlnB. It is plausible that after dephosphorylation by AlnB, the reaction may be nonenzymatic.

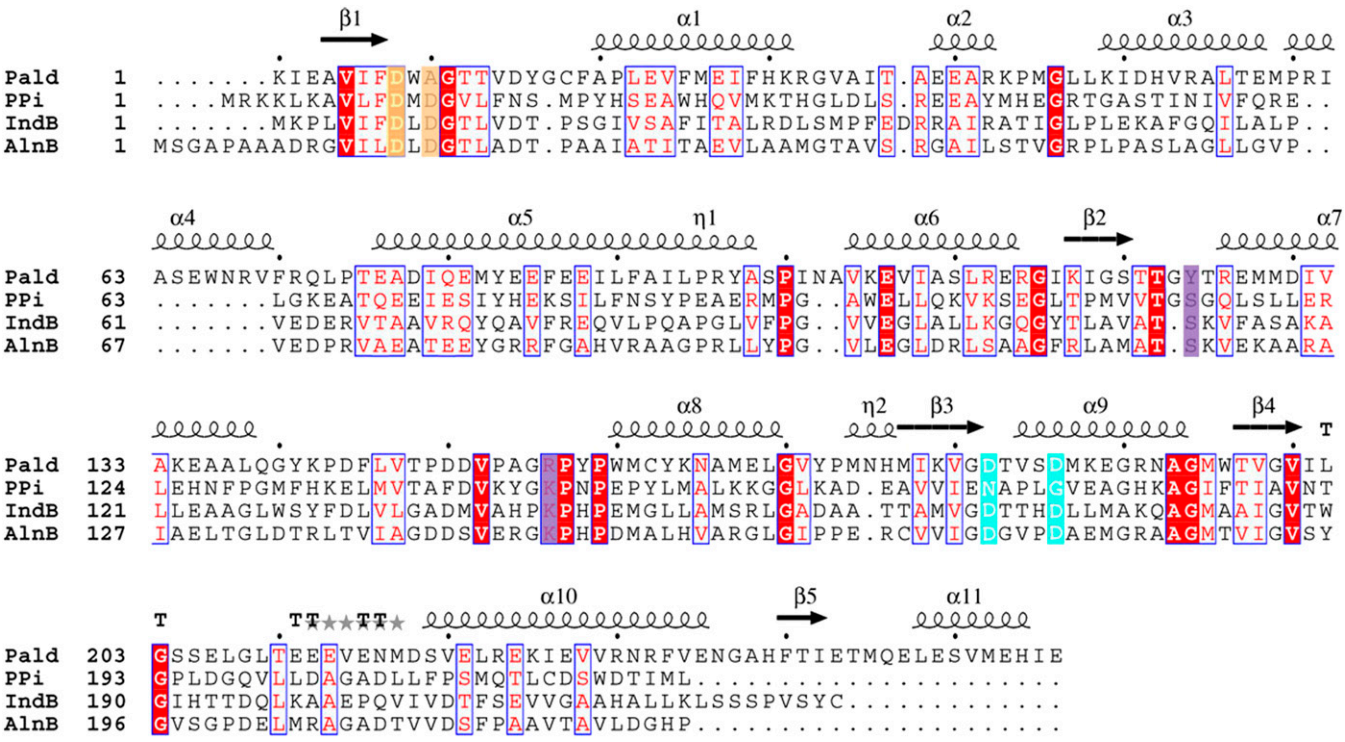


**Fig. S9.** Structure-based multiple sequence alignment of AlnB with related subfamily I members. The proteins included are the phosphonoacetaldehyde hydrolase Pald, *Bacillus cereus*; pyrophosphatase (PPi) BT2127, *Bacteroides thetaiotaomicron*; protein putatively involved in the biosynthesis of the pigment indigoidine IndB, *Erwinia chrysanthemi*. Amino acid residues that are conserved (red line), involved in catalysis (orange line), coordinating to the metal ion (cyan line), or the phosphate group of the cosubstrate (purple line) are shown. Only one of the catalytic aspartate residues is conserved in Pald (1).

1. Zhang G, et al. (2004) Investigation of metal ion binding in phosphonoacetaldehyde hydrolase identifies sequence markers for metal-activated enzymes of the HAD enzyme superfamily. *Biochemistry* 43(17):4990–4997.

**Table S1. X-ray data collection and crystallographic refinement statistics**

| Data collection | AlnA (native) | AlnA-5RP | AlnB (native) | AlnB + Pi |
|---|---|---|---|---|
| PDB entry | | | | |
| X-ray source | ESRF ID23-1 | ESRF ID23-2 | ESRF BM14 | ESRF ID14-2 |
| Space group | $I4_132$ | $I4_132$ | $P2_12_12_1$ | $P2_12_12_1$ |
| Unit cell (Å) | $a = b = c = 168.9$ | $a = b = c = 168.8$ | 48.0 62.9 63.2 | 48.3 63.2 63.5 |
| Resolution (Å) | 83.9–2.1 (2.21–2.10) | 50–3.15 (3.32–3.15) | 38.1–1.25 (1.32–1.25) | 38.4–1.5 (1.58–1.50) |
| Wavelength (Å) | 0.979 | 0.8726 | 1.072 | 0.933 |
| No. of unique reflections | 23665 | 7 414 | 46971 | 31272 |
| Multiplicity | 6.0 (6.1) | 7.7 (7.9) | 7.8 (5.8) | 3.0 (3.8) |
| Completeness (%) | 99.4 (100.0) | 100.0 (100.0) | 89.1 (53.4) | 98.4 (90.1) |
| Mean ($\langle I \rangle / \langle \sigma_I \rangle$) | 12.5 (2.8) | 10.1 (2.5) | 25.2 (7.5) | 11.2 (3.8) |
| R-sym (%)* | 7.8 (56.5) | 15.4 (80.7) | 4.7 (18.1) | 11.4 (21.1) |
| Wilson B-factor (Å$^2$) | 37.4 | 72.3 | 9.7 | 12.9 |
| Refinement | | | | |
| R-factor (all reflections) (%) | 17.2 | 22.0 | 11.9 | 14.4 |
| R-free (%)† | 20.0 | 24.8 | 15.3 | 18.6 |
| No. of atoms | 2362 | 2211 | 2024 | 1879 |
| No. of water molecules | 136 | 2 | 360 | 234 |
| No. of other molecules | 2 CA, CL, $SO_4$, 2 PEG | 5RP, 2 CA, CL, EPE | MG, $BO_3$ | MG, $BO_3$, $PO_4$ |
| RMSD bond lengths (Å) | 0.022 | 0.004 | 0.020 | 0.011 |
| RMSD bond angles (°) | 1.668 | 0.873 | 1.842 | 1.515 |
| Average B-factor (Å$^2$) | | | | |
| All atoms | 47.9 | 76.9 | 14.0 | 14.4 |
| Protein | 47.8 | 77.1 | 10.6 | 12.6 |
| Water/other molecules | 47.3/CA 45.0/ CL 72.5/ SO4 27.5/PEG 70.7 | 58.1/5RP 67.2/ CA 76.4/ CL 71.7/EPE 62.6 | 28.0/MG 6.1/ $BO_3$ 8.0 | 28.7/MG 5.6/ $BO_3$ 9.3/$PO_4$ 16.6 |
| Ramachandran plot | | | | |
| Favored regions (%) | 294 (96.1) | 295 (98.3) | 199 (98.5) | 197 (99.0) |
| Allowed regions (%) | 11 (3.6) | 5 (1.7) | 3 (1.5) | 2 (1.0) |
| Outliers (%) | 1 (0.3) | 0 | 0 | 0 |

Values in parenthesis are for the highest resolution shell. $BO_3$, boric acid; CA, calcium; CL, chloride; EPE, Hepes; MG, magnesium; PEG, polyethylene glycol; $PO_4$, phosphate; $SO_4$, sulfate; 5RP, D-ribulose-5-phosphate.

*R-sym = $[\sum_h \sum_i |I_i(h) - \langle I(h) \rangle| / (\sum_h \sum_i I(h))]$, where $I_i(h)$ is the $i$th measurement of reflection h and $\langle I(h) \rangle$ is the weighted mean of all measurements of h.

†5% of the reflections were used in the R-free calculations.

**Table S2. Oligonucleotide primers used in this study for cloning and mutagenesis**

| Primer | Sequence (5′→3′) |
|---|---|
| pBADseqfor | CGCAACTCTCTACTGTTTCTCC |
| pBADseqrev | GCGTTCTGATTTAATCTGTATCAGG |
| pBla7ABfor | TACCTGATGAAGGCGCTCGCCA |
| pBla7ABrev | CTAAAGGGAACAAAAGCTGGAGCTCC |
| alnAmutfor | GTTTCTCTTGAGGACCGCTGCGGC |
| alnAmutrev | CGGCCTTGGGCAGCATGC |
| alnBBfor | CAG**AGATCT**AGCGGCGCCCCCGC |
| alnBErev | CAG**GAATTC**GTTCACGGGTGTCCGTCCAG |
| alnAE29Afor | GTGGTGGCGCTGGCGTCCTCGCTCATC |
| alnAE29Arev | GATGAGCGAGGACGCCAGCGCCACCAC |
| alnAE29Qfor | GTGGTGGCGCTGCAGTCCTCGCTCATC |
| alnAE29Qrev | GATGAGCGAGGACTGCAGCGCCACCAC |
| alnAD138Afor | GAGGACACCCTCGCCATCTCCCCCGAC |
| alnAD138Arev | GTCGGGGGAGATGGCGAGGGTGTCCTC |
| alnAK159Rfor | CTCCGGCGGCGCGAGAAGCATCCTGGACC |
| alnAK159Rrev | GGTCCAGGATGCTTCTCGCGCCGCCGGAG |
| alnAK86Afor | GGGCATTCCGGCGATCAGCGCGC |
| alnAK86Arev | GCGCGCTGATCGCCGGAATGCCC |
| alnAH130Afor | CGGCGGTGTGGCCCGCAGGGGCG |
| alnAH130Arev | CGCCCCTGCGGGCCACACCGCCG |
| alnAK159Afor | CGGCGGCGCGGCGAGCATCCTGG |
| alnAK159Arev | CCAGGATGCTCGCCGCGCCGCCG |
| alnBD15Afor | CCTCGCGCTCGACGGCACACTC |
| alnBD15Arev | GAGTGTGCCGTCGAGCGCGAGG |
| alnBD15Nfor | CCTCAACCTCGACGGCACACTC |
| alnBD15Nrev | GAGTGTGCCGTCGAGGTTGAGG |
| alnBD17Afor | CCTCGACCTCGCCGGCACACTC |
| alnBD17Arev | GAGTGTGCCGGCGAGGTCGAGG |
| alnBY79Afor | GACCGAGGAGGCGGGGCGGCG |
| alnBY79Arev | CGCCGCCCCGCCTCCTCGGTC |
| alnBK119Afor | CGACCTCGGCGGTCGAGAAGGCC |
| alnBK119Arev | GGCCTTCTCGACCGCCGAGGTCG |
| alnBK119Rfor | CGACCTCGAGGGTCGAGAAGGCC |
| alnBK119Rev | GGCCTTCTCGACCCTCGAGGTCG |

Recognition sites of the restriction endonucleases BglII and EcoRI used in cloning are shown in bold.

**Table S3. Partial $^{1}H$ and $^{13}C$ NMR assignments of alnumycins P1 (4a) and P2 (4b) in $CD_3OD$ at 25 °C**

| | Alnumycin P1 (**4a**) | | | | Alnumycin P2 (**4b**) | | | |
|---|---|---|---|---|---|---|---|---|
| | δ/ppm | | | | δ/ppm | | | |
| Position | $^{13}C$ | $^{1}H$ | Mult. | $J_{H,H}$/Hz (spin partner) | $^{13}C$ | $^{1}H$ | Mult. | $J_{H,H}$/Hz (spin partner) |
| 1 | 74.1 | 5.63 | app dd | 9.39 (H-11a); 3.56 (H-11b) | ol | ol | | |
| 3 | 159.5 | — | | | ol | — | | |
| 4 | 101.0 | 5.74 | qt | 0.88 (H-14) | ol | ol | | |
| 4a | 123.1 | — | | | ol | — | | |
| 5 | 108.6 | 7.01 | br s | | ol | ol | | |
| 5a | 133.2 | — | | | 135.4 | — | | |
| 6 | 186.7 | — | | | no | — | | |
| 7 | 135.4 | 7.11 | d | 1.66 (H-1′) | 135.8 | 6.93 | d | 1.90 (H-1′) |
| 8 | 151.3 | — | | | no | — | | |
| 9 | 190.2 | — | | | no | — | | |
| 9a | no | — | | | no | — | | |
| 10 | no | — | | | no | — | | |
| 10a | 114.9 | — | | | ol | — | | |
| 11 | 35.9 | 2.02, 1.50 | m | | ol | ol | | |
| 12 | 19.3 | 1.57, 1.49 | m | | ol | ol | | |
| 13 | 14.1 | 0.97 | app t | 7.17 (2 × H-12) | ol | ol | | |
| 14 | 20.3 | 1.95 | d | 0.88 (H-4) | ol | ol | | |
| 1′ | 80.7 | 5.01 | dd | 3.48 (H-2′); 1.66 (H-7) | 79.3 | 5.20 | dd | 3.63 (H-2′); 1.90 (H-7) |
| 2′ | 77.7 | 4.10 | ol | | 74.7 | 4.49 | dd | 4.58 (H-3′); 3.63 (H-1′) |
| 3′ | 72.5 | 4.09 | ol | | 73.9 | 4.42 | dd | 8.16 (H-4′); 4.58 (H-2′) |
| 4′ | 83.4 | 4.10 | ol | | 82.2 | 4.05 | ol | |
| 5′ | 66.5 | 4.14, 4.08 | ol | | 65.7 | 4.14, 4.08 | ol | |
| P | 4.75 | — | | ho t, ~ 5.8 | ol | — | | ol |

The chemical shifts of $^{1}H$ and $^{13}C$ nuclei are reported relative to TMS as an internal standard (δ = 0 ppm for both $^{1}H$ and $^{13}C$) and externally to 90% $H_3PO_4$ in $D_2O$ for $^{31}P$. app, apparent; br, broad or broadened; d, doublet; dd, doublet of doublets; ho, higher order; ol, overlapped; m, multiplet; no, not observed; qt, quartet; s, singlet; t, triplet.